



# Ultra-low-dose coronary computed tomography angiography using photon-counting detector computed tomography

Suguru Araki <sup>1</sup>, Satoshi Nakamura <sup>2,\*</sup>, Masafumi Takafuji<sup>1</sup>, Yasutaka Ichikawa<sup>1</sup>, Hajime Sakuma<sup>1</sup>, and Kakuya Kitagawa<sup>2,3</sup>

<sup>1</sup>Department of Radiology, Mie University Hospital, Tsu, Japan

<sup>2</sup>Department of Advanced Diagnostic Imaging, Mie University Graduate School of Medicine, 2-174 Edobashi, Tsu, Mie 514-8507, Japan

<sup>3</sup>Regional Co-creation Deployment Center, Mie Regional Plan Co-creation Organization, Mie University, Tsu, Japan

Received 1 October 2024; accepted after revision 14 November 2024; online publish-ahead-of-print 27 November 2024

## Abstract

### Aims

Photon-counting detector computed tomography (PCD-CT), which allows the exclusion of electronic noise, shows promise for significant dose reduction in coronary CT angiography (CCTA). This study aimed to assess the radiation dose and image quality of CCTA using PCD-CT, combined with high-pitch helical scanning and an ultra-low tube potential of 70 kVp, and investigate the effect of a sharp kernel on image quality and stenosis assessment in such an ultra-low-dose CCTA setting.

### Methods and results

Forty patients (65% male) with stable heart rates and no prior coronary interventions were included. Data on CT dose index volume (CTDIvol) and dose-length product (DLP) were collected, with effective radiation dose estimated using a conversion factor of 0.014. Images were reconstructed using kernels of Bv64 and Bv40 for image quality and stenosis assessment. The mean CTDIvol, DLP, and effective dose of CCTA were  $1.72 \pm 0.38$  mGy,  $29.1 \pm 6.8$  mGy·cm, and  $0.41 \pm 0.09$  mSv, respectively. Image quality was similar ( $P = 0.75$ ) between the two kernels, with over 95% of segments achieving a rating of good image quality for both kernels. The per-segment stenosis score distribution between Bv40 and Bv64 reconstruction images showed significant differences for both non-calcified and calcified plaques ( $P < 0.001$  for both).

### Conclusion

PCD-CT technology with high-pitch helical scanning and the tube potential of 70 kVp can provide CCTA with ultra-low radiation exposure (DLP, 29 mGy·cm). The noise reduction capability of PCD-CT allows the use of a sharp kernel even in this low-dose CCTA setting without compromising image quality, potentially improving the evaluation of coronary artery stenosis.

\* Corresponding author. E-mail: [s-nakamura@med.mie-u.ac.jp](mailto:s-nakamura@med.mie-u.ac.jp)

© The Author(s) 2024. Published by Oxford University Press on behalf of the European Society of Cardiology.

This is an Open Access article distributed under the terms of the Creative Commons Attribution-NonCommercial License (<https://creativecommons.org/licenses/by-nc/4.0/>), which permits non-commercial re-use, distribution, and reproduction in any medium, provided the original work is properly cited. For commercial re-use, please contact [reprints@oup.com](mailto:reprints@oup.com) for reprints and translation rights for reprints. All other permissions can be obtained through our RightsLink service via the Permissions link on the article page on our site—for further information please contact [journals.permissions@oup.com](mailto:journals.permissions@oup.com).

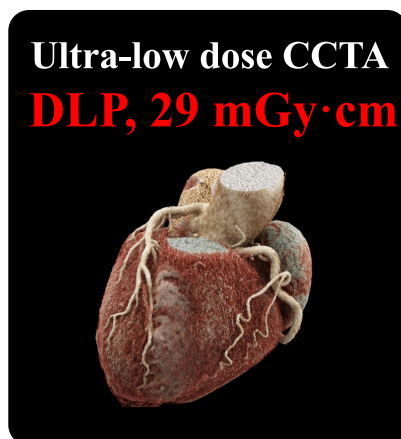
## Graphical Abstract

## Ultra-low dose CCTA using PCD-CT in conjunction with high-pitch helical scan and ultra-low tube potential

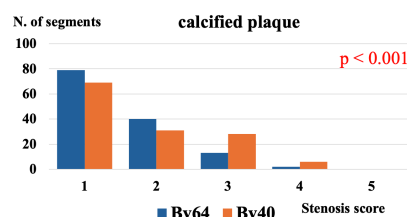
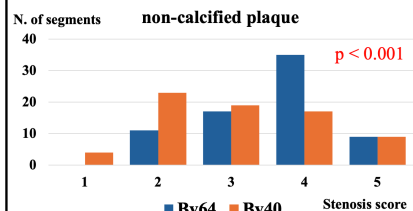
High-pitch helical scan by dual-source CT

Reduction of electronic noise by PCD

Ultra-low tube potential (70kVp)



### Effect of kernels on stenosis assessment



The noise reduction capability of PCD-CT allows the use of a sharp kernel even in ultra-low dose CCTA without compromising image quality, potentially improving the evaluation of coronary artery stenosis.

### Keywords

coronary arteries • computed tomography angiography • photon-counting CT • dual-source CT • low radiation exposure

## Introduction

Cardiac computed tomography (CT) is widely used as a non-invasive imaging modality in clinical practice.<sup>1,2</sup> Coronary CT angiography (CCTA) can rule out coronary artery disease (CAD) with a high negative predictive value<sup>3</sup> and provides significant prognostic information, leading to a substantial reduction in cardiac deaths or non-fatal myocardial infarctions.<sup>4,5</sup> However, as its availability in daily clinical practice has expanded, concerns over the radiation dose from CCTA have increased.<sup>6</sup> Radiographic examinations, including cardiac CT, should be optimized to maintain diagnostic image quality while ensuring the dose is 'as low as reasonably achievable'.<sup>7</sup>

CCTA was often performed, or is sometimes performed, using electrocardiogram (ECG)-gated retrospective helical scanning, which can result in high radiation exposure (sometimes exceeding 30 mSv).<sup>8</sup> However, various dose-reduction techniques have been developed, including adjusting the tube potential based on patient size (reducing exposure by up to 45%),<sup>9</sup> ECG-based tube current modulation (reducing exposure by ~40%),<sup>10</sup> and ECG-triggered prospective axial acquisition for patients with stable, low heart rates, achieving doses below 5 mSv.<sup>11,12</sup> Additionally, since 2005, dual-source CT technology has enabled ECG-triggered high-pitch helical scanning, which allows whole-heart imaging in a fraction of a cardiac cycle with very low radiation exposure (~1 mSv).<sup>13,14</sup>

Recently, photon-counting detector CT (PCD-CT) scanners with dual-source CT technology have entered clinical practice. Compared with conventional energy-integrating detectors (EIDs), PCDs provide higher spatial resolution and photon efficiency, which contribute to improved image

quality and reduced radiation dose.<sup>15</sup> PCD systems can exclude electronic noise by setting an energy threshold slightly higher than the energy level associated with the electronic noise signal, thus improving the signal-to-noise ratio (SNR) and potentially allowing for lower radiation doses.<sup>16</sup> Although the combination of PCD technology with ECG-triggered prospective high-pitch helical scanning by dual-source technology and ultra-low tube potential of 70 kVp may enable CCTA with extremely low radiation exposure, the effectiveness of this approach has yet to be investigated.

The choice of reconstruction kernel plays a crucial role in the assessment of coronary arteries and plaques. According to Mergen et al.,<sup>17</sup> the ability of PCD-CT to exclude the electronic noise enables the use of sharper kernels compared with EID-CT, potentially allowing more accurate quantification of coronary plaques. However, the use of sharper kernels can result in increased image noise. While extremely low-dose CCTA may inherently increase more noise compared with higher-dose CCTA, it remains uncertain whether the advantages of using sharper kernels can be fully realized at such low dose without being offset by the associated drawbacks. Furthermore, the extent to which differences in reconstruction kernels affect not only plaque volume measurement but also the evaluation of stenosis severity remains unclear.

Therefore, the aim of this study was to evaluate the radiation dose and image quality of CCTA using PCD-CT in conjunction with ECG-triggered prospective high-pitch helical scanning and the ultra-low tube potential of 70 kVp. Additionally, we aimed to determine whether image quality can be maintained when applying a sharp kernel compared with a smooth kernel in such CCTA and whether there are

any differences in the degree of coronary artery stenosis assessed between CCTA images obtained using these two kernels.

## Methods

### Study design

This research was conducted as a retrospective study, focusing on the assessment of a novel CCTA technique that combined a high-pitch helical scan with an ultra-low tube potential of 70 kVp using a PCD-CT scanner. The institutional review board in our hospital approved the protocols for this study and waived the need to obtain individual consent based on the retrospective design.

We analysed CCTA performed with ECG-triggered prospective high-pitch helical acquisition and ultra-low tube potential of 70 kVp using a PCD-CT scanner between October 2023 and July 2024 at our hospital. The study enrolled patients with known or suspected CAD who had no history of coronary artery stent implantation or bypass grafting. Eligibility also required a heart rate below 65 bpm with stable sinus rhythm. Accordingly, 44 patients who met these criteria were included. The study excluded patients with congenital heart disease ( $n = 3$ ) or the presence of an implantable cardioverter defibrillator ( $n = 1$ ). Patients were not excluded based on heart rate variability, body weight, or body mass index (BMI). Consequently, the final study cohort consisted of 40 patients.

### Image acquisition

All scans in this study were performed using a first-generation dual-source PCD-CT scanner (NAEOTOM Alpha, Siemens Healthineers, Forchheim, Germany). The patient lied supine in the scanner and attached to an ECG monitor and automated blood pressure monitor. After anteroposterior and lateral topograms, unenhanced CT images for coronary artery calcium scoring were performed using ECG-triggered prospective high-pitch helical scan at 100 kV with a Sn filter. CCTA with ECG-triggered prospective high-pitch helical mode (Turbo Flash) was performed with a starting phase of 70% R-R interval by bolus injection of 26 mg/kg/s of iopamidol (Iopamilon-370, Bayer AG, Leverkusen, Germany) over 12 s, followed by a 20 mL saline flush, with the coronary arteries dilated with a sublingual nitrate (Myocor sprays,

Toa Eiyo Co., Ltd, Tokyo, Japan). Heart rate was controlled before CCTA with intravenous injection of landiolol hydrochloride (Corebeta, Ono Pharmaceutical Co., Ltd, Osaka, Japan), if necessary. The acquisition parameters of CCTA were as follows: a pitch factor of 3.2, collimation of 144 mm  $\times$  0.4 mm, gantry rotation time of 0.25 s, and tube voltage of 70 kV. Automatic exposure control (CAREkeV, Siemens Healthineers, Forchheim, Germany) was utilized. Tube current was set by the CT scanner automatically to achieve a target CT dose index volume (CTDIvol), which was  $\sim 2$  mGy. Data for each patient, including effective mAs, were shown in [Supplementary data online, Table S1](#). Axial images of CCTA were reconstructed with a slice thickness and increment of 0.4/0.2 mm, monoenergetic energy level of 53 keV, quantum iterative reconstruction level of 4, vascular convolution kernel (Bv64 and Bv40), image matrix of 512  $\times$  512, and a field of view restricted to the heart.

### Subjective image quality analysis

Two radiologists, with 4 (S.A.) and 10 (S.N.) years of experience in cardiovascular imaging, conducted a consensus reading to visually assess the image quality of the CCTA data. The observers used the following 4-point scale for the visual assessment, considering factors such as motion artefacts, sharpness, noise, contrast enhancement, and beam hardening, which are crucial for analysing the morphology of coronary arteries and plaque: (i) non-diagnostic (the image quality is so poor that assessing the morphology of coronary arteries and plaque is impossible); (ii) fair (the image quality poses some challenges, but morphology assessment is still feasible); (iii) good (the image quality presents minor imperfections, yet allows for morphology assessment without major difficulties); and (iv) excellent (the image quality makes assessment straightforward and easy) ([Figure 1](#)).<sup>13,14</sup> In this visual assessment, the observers evaluated each segment of the coronary arteries based on the 18-segment model of the Society of Cardiovascular Computed Tomography.<sup>15</sup>

### Objective image quality analysis

Signal intensity, image noise, contrast-to-noise ratio (CNR), and SNR were quantified as objective image quality parameters. All measurements were performed (by S.A.) on reformatted axial images with a slice thickness of 0.4 mm. Signal intensity was derived from the mean CT attenuation values

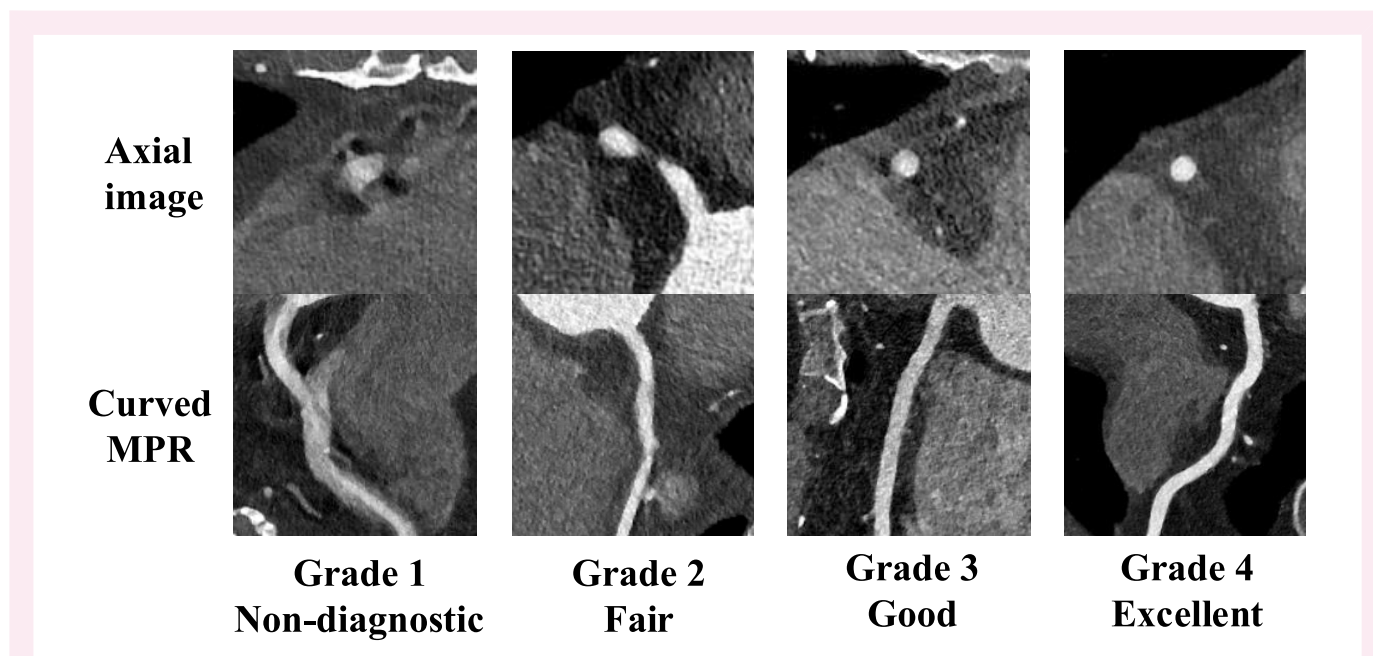


**Figure 1** Illustration of image quality scores of coronary arteries on CCTA images. The figures show a 4-point scale used to assess the image quality of the CCTA images: (1) non-diagnostic; (2) fair; (3) good; and (4) excellent. CCTA, coronary computed tomography angiography; MPR, multiplanar reconstruction.

[Hounsfield units (HU)] averaged from two circular regions of interest (size 3–4 mm<sup>2</sup>) in the proximal segments of the left and right coronary artery lumen. Image noise was defined as the averaged standard deviations of the CT attenuation values within these two regions of interest. We calculated the difference between the mean CT attenuation values of the proximal coronary arteries and the mean CT attenuation value of the left ventricular lateral wall and defined the CNR as the difference divided by image noise. The SNR was calculated as mean CT attenuation values of the left and right coronary arteries divided by the image noise.<sup>19</sup>

## Coronary stenosis severity assessment

The severity of coronary stenosis was assessed on a per-segment basis through consensus reading by two readers (S.A. and S.N.) in both Bv64 and Bv40 reconstruction CCTA images using the following scoring system: 0 (0%), 1 (1–24%), 2 (25–49%), 3 (50–69%), 4 (70–99%), and 5 (100%).<sup>20</sup> Each plaque was classified as non-calcified plaque or calcified plaque based on whether the calcification or non-calcification component was predominant. For each segment, only the maximum stenosis score was recorded.

## Radiation dose estimation

The CTDIvol and dose-length product (DLP) were extracted from the participant protocols. The effective dose was calculated by multiplying the DLP by a conversion factor of 0.014 mSv/mGy·cm.

## Statistical analysis

Statistical analysis was carried out using JMP14.2.0 (SAS, Institute Cary, NC, USA) software. The primary metrics of interest were the effective radiation dose, calculated using the DLP, and qualitative and quantitative assessments for image quality. Descriptive statistics (mean and standard deviation) were used to summarize the data. Qualitative and quantitative image quality was compared between Bv40 and Bv64 CCTA images using either the  $\chi^2$  test or t-test, as appropriate. The severity of stenosis for each coronary plaque was assessed between Bv40 and Bv64 CCTA images using the Wilcoxon signed-rank test. A *P*-value of <0.05 was considered statistically significant.

## Results

Patient characteristics and CCTA parameters are listed in Table 1. Of the 40 patients, 26 were male and 14 were female. The mean age was 73 ± 12. The mean body weight was 58.0 ± 9.6 kg (range:

41.0–85.9 kg) and the mean BMI was 22.3 ± 3.0 kg/m<sup>2</sup> (range: 17.8–28.0 kg/m<sup>2</sup>). The mean heart rate during the scan was 56 ± 5 bpm (range: 45–64 bpm). The mean CTDIvol and DLP of the CCTA was 1.72 ± 0.38 mGy (range: 0.72–2.13 mGy) and 29.1 ± 6.8 mGy·cm (range: 11.0–38.4 mGy·cm), respectively. They corresponded to an estimated effective dose of 0.41 ± 0.09 mSv (range: 0.15–0.54 mSv).

Image quality of CCTA images is listed in Table 2. A total of 596 coronary artery segments were analysed. Of those, 483 segments (81.0%) had an image quality score of 4 ('excellent'), 88 segments (14.8%) a score of 3 ('good'), 17 segments (2.9%) a score of 2 ('fair'), and 8 segments (1.3%) were scored as 1 ('non-diagnostic') on Bv64 reconstruction, whereas 490 segments (82.2%) had an image quality score of 4, 88 segments (14.8%) a score of 3, 12 segments (2.9%) a score of 2, and 6 segments (1.0%) a score of 1 on Bv40 reconstruction. Mean rating scores for all segments of Bv64 and Bv40 reconstruction image were 3.76 and 3.78, respectively. On Bv64 reconstruction, signal intensity and image noise were 884.7 ± 157.7 and 110.8 ± 15.0 HU, respectively. CNR and SNR were 6.8 ± 1.7 and 8.1 ± 1.7, respectively. On Bv40 reconstruction, signal intensity and image noise were 867.9 ± 155.8 and 40.9 ± 9.8 HU, respectively. CNR and SNR were 18.7 ± 5.5 and 22.2 ± 6.0, respectively. A representative case of CCTA in this study is given in Figure 2. Figure 3 displays CCTA images with the lowest level of radiation exposure (0.15 mSv).

Figure 4 presents the differences in coronary plaque appearance between Bv64 and Bv40 in representative cases, and a representative image of the aorta (Figure 5) shows the differences in image noise between the two convolution kernels. In the assessment of non-calcified plaque, the Bv64 reconstruction showed the following distribution of coronary stenosis scores: 0 cases with a score of 1, 11 cases with a score of 2, 17 cases with a score of 3, 35 cases with a score of 4, and 9 cases with a score of 5. In contrast, the Bv40 reconstruction demonstrated 4 cases with a score of 1, 23 cases with a score of 2, 19 cases with a score of 3, 17 cases with a score of 4, and 9 cases with a score of 5 (Figure 6A). The distribution of stenosis scores for non-calcified plaques was significantly different (*P* < 0.001) between the Bv64 and Bv40 reconstruction images based on the Wilcoxon signed-rank test.

For calcified plaque, the Bv64 reconstruction revealed 79 cases with a score of 1, 40 cases with a score of 2, 13 cases with a score of 3, 2 cases with a score of 4, and 0 cases with a score of 5. Meanwhile, the Bv40 reconstruction showed 69 cases with a score of 1, 31 cases with a score of 2, 28 cases with a score of 3, 6 cases with a score of 4, and 0 cases with a score of 5 (Figure 6B). The distribution of stenosis

**Table 1 Patient characteristics, CCTA parameters, and image quality of CCTA images**

All participants (n = 40)	
Patient characteristics	
Male, n (%)	26 (65)
Age (years)	73 ± 12
Body weight (kg)	58.0 ± 9.6
BMI (kg/m <sup>2</sup> )	22.3 ± 3.0
CCTA parameters	
Heart rate (bpm)	56 ± 5
Amount of contrast (mL)	51.4 ± 7.2
Flow rate (mL/s)	4.3 ± 0.6
CTDIvol (mGy)	1.72 ± 0.38
DLP (mGy · cm)	29.1 ± 6.8
Effective dose (mSv)	0.41 ± 0.09

Data are presented as the mean ± standard deviation or number of patients (%). BMI, body mass index; CCTA, coronary computed tomography angiography; CTDIvol, computed tomography dose index volume; DLP, dose-length product.

**Table 2 Image quality of CCTA images (Bv64 and Bv40)**

	Bv64 (n = 40)	Bv40 (n = 0)	<i>P</i> -value
Image quality score			0.75
1. Non-diagnostic, n (%)	8 (1.3)	6 (1.0)	
2. Fair, n (%)	17 (2.9)	12 (2.0)	
3. Good, n (%)	88 (14.8)	88 (14.8)	
4. Excellent, n (%)	483 (81.0)	490 (82.2)	
Signal intensity (HU)	884.7 ± 157.7	867.9 ± 155.8	0.63
Image noise (HU)	110.8 ± 15.0	40.9 ± 9.8	<0.0001
Contrast-to-noise ratio	6.8 ± 1.7	18.7 ± 5.5	<0.0001
Signal-to-noise ratio	8.1 ± 1.7	22.2 ± 6.0	<0.0001

Data are presented as the mean ± standard deviation or number of patients (%). HU, Hounsfield unit.



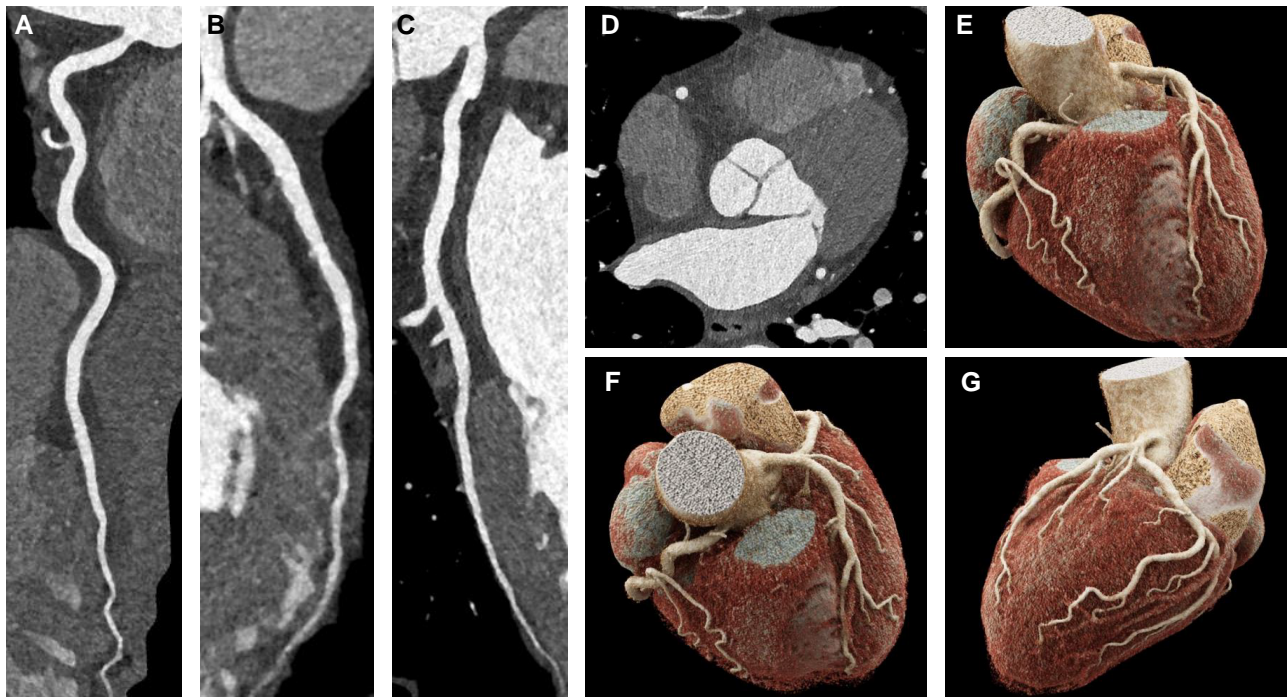


**Figure 2** A representative case of ultra-low-dose CCTA. The figures show CCTA images of a 69-year-old male (160 cm, 61 kg), which were obtained with ECG-triggered prospective high-pitch helical acquisition (pitch, 3.2) and ultra-low tube potential of 70 kVp using a photon-counting detector CT scanner. The heart rate during the scan was 56 bpm. The CTDIvol and DLP for CCTA was 1.97 mGy and 32.6 mGy·cm (estimated effective dose 0.46 mSv), respectively. No coronary artery stenoses are present on CCTA images. (A) Curved multiplanar reconstruction of right coronary artery. (B) Curved multiplanar reconstruction of left anterior descending coronary artery. (C) Curved multiplanar reconstruction of left circumflex coronary artery. (D) Transaxial image (0.4 mm slice thickness) at the level of the mid-right coronary artery. (E–G) Cinematic volume rendering image of the heart and coronary arteries. CCTA, coronary computed tomography angiography; ECG, electrocardiogram; CTDIvol, computed tomography dose index volume; DLP, dose-length product.

scores for calcified plaques was significantly different ( $P < 0.001$ ) between the Bv64 and Bv40 reconstruction images based on the Wilcoxon signed-rank test.

Figure 6C and D illustrates the changes in the stenosis score between the Bv64 and Bv40 kernels for non-calcified and calcified plaques, respectively. Some non-calcified plaque had an increased stenosis score from Bv40 to Bv64 images, and some calcified plaque had a decreased score.

## Discussion

The study was the first one that performed CCTA by ECG-triggered prospective high-pitch helical scan protocol (FLASH) in combination with ultra-low tube potential of 70 kVp using PCD-CT scanner to assess radiation dose and image quality of this technique. The study showed that this new technique provided CCTA with an extremely low effective radiation dose of  $\sim 0.4$  mSv and high-quality images. The use of a sharp kernel in this low-dose CCTA setting may allow improved evaluation of coronary artery stenosis by reducing the overestimation of stenosis in calcified plaques and the underestimation in non-calcified plaques.

Several techniques have been developed to reduce radiation exposure during CCTA. These include prospective ECG-triggering, high-pitch scanning, reducing tube voltage, adjusting tube current, ECG-controlled tube current modulation, and iterative reconstruction. The effectiveness of these efforts has been recognized in various

surveys, such as the PROTECTION VI study,<sup>21</sup> where a comparison of data from 2007 and 2017 revealed a 78% reduction in radiation exposure of CCTA across different clinical sites, although it also pointed out the need for further site-specific training and adaptation to optimize the use of dose-saving techniques.

The ECG-triggered prospective high-pitch helical scan needs high temporal resolution and a relatively long diastolic window of cardiac cycle, although it can provide images with high image quality free from stair-step artefacts and extremely low radiation exposure in CCTA. Dual-source CT technology has high temporal resolution because it compensates for gaps in the first detector's trajectory, which are caused by rapid table motion, using a second detector. There are some reports concerning the usefulness of ECG-triggered prospective high-pitch helical scan by the second-generation dual-source CT (SOMATOM Definition Flash). Lell *et al.* analysed 25 consecutive patients with stable heart rates of 60 bpm or less who underwent this scanning technique. All scans were performed with tube potential of 100 or 120 kVp. They demonstrated that the mean DLP was  $71 \pm 23$  mGy·cm and the mean effective dose was  $1.0 \pm 0.3$  mSv (range: 0.78–2.1 mSv). The mean DLP was  $63 \pm 5$  mGy·cm and mean effective dose was  $0.88 \pm 0.07$  mSv (range: 0.78–0.97 mSv) for the 21 patients with a body weight below 100 kg.<sup>22</sup> Achenbach *et al.* have also analysed 50 consecutive patients with stable heart rates of 60 bpm or less and body weight of 100 kg or below who underwent ECG-triggered prospective high-pitch helical scan with tube potential set at 100 kVp. They reported that the mean DLP was  $62 \pm$

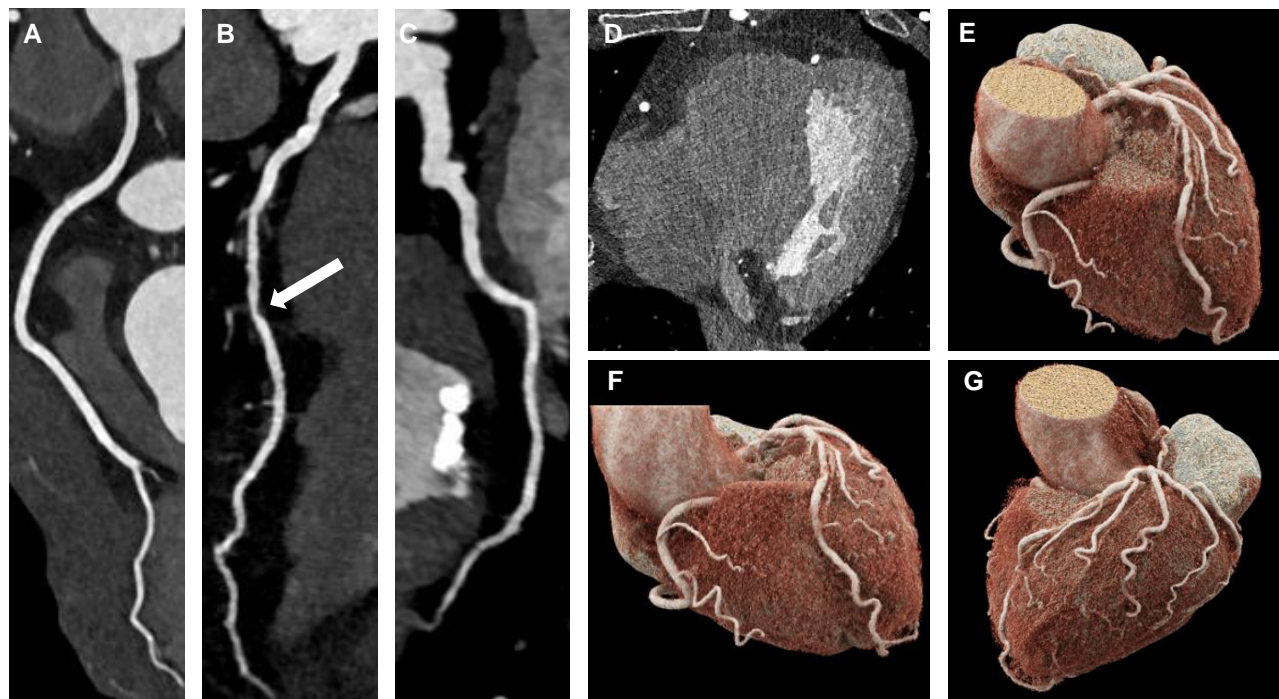


**Figure 3** CCTA images with the lowest level of radiation exposure. The figures show CCTA images of an 81-year-old female (145 cm, 42 kg), which were obtained with ECG-triggered prospective high-pitch helical acquisition (pitch, 3.2) and ultra-low tube potential of 70 kVp using a photon-counting detector CT scanner. The heart rate during the scan was 64 bpm. The CTDIvol and DLP for CCTA was 0.72 mGy and 11.0 mGy·cm (estimated effective dose 0.15 mSv), respectively. (A) Curved multiplanar reconstruction of right coronary artery. (B) Curved multiplanar reconstruction of left anterior descending coronary artery, which displays a moderate stenosis in the mid segment (arrow). (C) Curved multiplanar reconstruction of left circumflex coronary artery. (D) Transaxial image (0.4 mm slice thickness) at the level of the mid-right coronary artery. (E–G) Cinematic volume rendering image of the heart and coronary arteries. CCTA, coronary computed tomography angiography; ECG, electrocardiogram; CTDIvol, computed tomography dose index volume; DLP, dose-length product.

5 mGy·cm and the mean effective dose was  $0.87 \pm 0.07$  mSv (range: 0.78–0.99 mSv).<sup>14</sup> Both studies reported that CCTA with ECG-triggered prospective high-pitch helical scan was feasible and provided excellent image quality with a mean effective radiation dose of over 0.8 mSv. Our research advanced CCTA by performing this high-pitch helical scan in conjunction with an ultra-low tube potential of 70 kVp using the PCD-CT, achieving an unprecedented mean effective radiation dose ( $\sim 0.4$  mSv).

PCD-CT represents a significant advancement in CT, offering substantial improvements in image quality and noise reduction. This technology, which directly converts X-ray photons into electronic signals, allows for ultra-high-resolution imaging and superior SNR by effectively eliminating electronic noise. Studies have shown that PCD-CT can achieve considerable reductions in image noise compared with conventional EID-CT, even at lower radiation doses.<sup>23</sup> These improvements in image quality and noise reduction, as recent studies have reported, have been useful in the field of cardiovascular imaging.<sup>24</sup> There are very few reports of CCTA of ECG-triggered prospective high-pitch helical scan with PCD-CT. Rotkopf et al. retrospectively analysed 73 patients who underwent ECG-triggered prospective high-pitch helical scan with PCD-CT. They found that the ultra-fast acquisition speed and high temporal resolution of PCD-CT allowed for robust image quality even in patients with higher heart rates or heart rate variability. The mean DLP of CCTA was  $56.5 \pm 24.8$  mGy·cm, of which the mean effective dose was  $0.79 \pm 0.35$  mSv (estimated by conversion factor 0.014).<sup>25</sup> Another study using high-pitch CCTA included 27 patients using a low contrast dose (30 mL of iohexol 350 mg/mL) and 26 patients using

a routine contrast dose (60 mL) and concluded that the high-pitch PCD-CT mode produced diagnostic quality CCTA images at low radiation and iodinated contrast doses, with the availability of virtual mono-energetic images significantly improving CNR and overall image quality.<sup>26</sup> The mean CTDI of CCTA in this study was  $2.8 \pm 1.2$  mGy, although the DLP was not reported. It is of note that all the scans in both studies were performed with tube potential of 120 kVp, and therefore, the radiation doses of those studies are not substantially reduced compared with EID-CT scanners with dual-source technology. As presented in Table 3, we have summarized the radiation dose data from this study alongside those from previous reports, detailing CTDIvol, DLP, and effective dose calculated with various conversion factors.<sup>13,14,22,25–29</sup> By employing an ultra-low tube potential of 70 kVp, our study takes full advantage of PCD-CT technology to achieve significant radiation dose reduction. This use of 70 kVp combined with high-pitch helical scan is beneficial in minimizing patient exposure to ionizing radiation, resulting in a mean CTDI of 1.7 mGy and a mean effective radiation dose of 0.4 mSv.

A study by Mergen et al.<sup>17</sup> evaluated the effects of using ultra-high-resolution PCD-CT for CCTA on quantitative plaque characterization in 20 patients with 22 coronary plaques. The study compared images reconstructed with a smooth (Bv40) and a sharp (Bv64) vascular kernel, finding that the sharp kernel (Bv64) provided more accurate quantification of plaques, with reduced blooming artefacts and improved visualization of non-calcified components. Despite increased image noise, the sharp kernel showed promise in enhancing the accuracy of coronary plaque assessment. Our study demonstrated

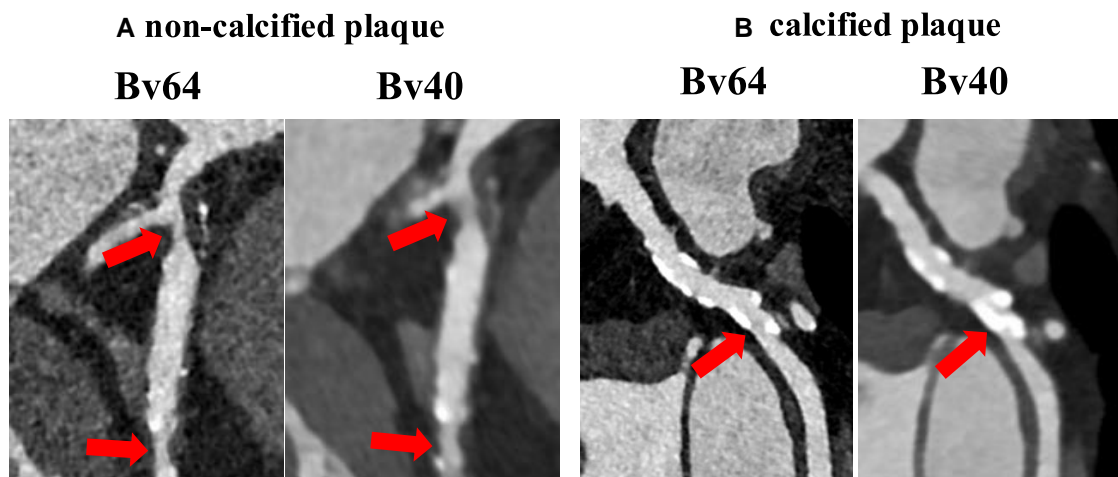


**Figure 4** Comparison of CCTA images reconstructed using Bv64 and Bv40 kernels. The figure presents representative CCTA images reconstructed using Bv64 and Bv40 kernels. (A) The images depict the proximal left anterior descending artery of an 84-year-old male, showing two non-calcified plaques (indicated by arrows). In the Bv64 kernel reconstruction image, the plaque margins are sharply delineated, with the stenosis evaluated as score 4 (70–99%). In contrast, the Bv40 kernel reconstruction image shows blurred plaque margins and vessel lumen, leading to a stenosis assessment of score 3 (50–69%). (B) The images show the proximal left circumflex artery of an 80-year-old male with a calcified plaque (indicated by the arrow). In the Bv64 kernel reconstruction image, calcification blooming is suppressed, and the plaque margin is sharply delineated, allowing for a clearer evaluation of the lumen. The stenosis is assessed as score 2 (25–49%). In contrast, in the Bv40 kernel reconstruction image, calcification blooming is more pronounced, resulting in a stenosis assessment of score 4 (70% to 99%). CCTA, coronary computed tomography angiography.

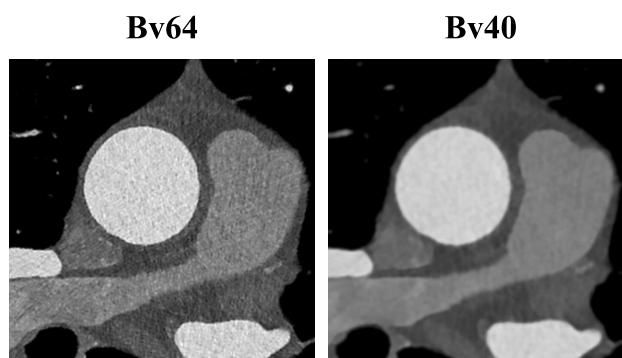


**Figure 5** Representative CCTA images at the level of the ascending aorta. These axial CCTA images of the ascending aorta illustrate that the Bv64 kernel exhibited slightly higher subjective image noise but provided superior sharpness compared with the Bv40 kernel.

that the evaluation of coronary artery stenosis may be improved with the sharp kernel, as it reduced the overestimation of stenosis in calcified plaques and the underestimation in non-calcified plaques. Importantly, the image quality was maintained with the sharp kernel, even in the context of ultra-low-dose CCTA.

This current study suggests several potential benefits. The ability to perform CCTA with an ultra-low radiation dose of 0.4 mSv is a major advancement in patient safety, as it minimizes the risk associated with ionizing radiation, making the procedure safer for patients, particularly those requiring multiple scans or follow-up studies. The high-quality imaging achieved with this technique, despite the low radiation dose, could allow for the broader use of CCTA in populations that are typically at higher risk from radiation exposure, such as young patients and women of childbearing age. Our results may also encourage the use of CCTA as a preventive screening tool for high-risk patients, aiding in the

early detection and management of CAD. Moreover, while some studies using EID-CT have suggested that the use of a low tube potential, such as 80 kVp, for CCTA is feasible only under certain conditions, such as a body weight below 60 kg or BMI below 25 kg/m<sup>2</sup>,<sup>30–32</sup> our cohort included patients with body weights above 60 kg or BMI above 25 kg/m<sup>2</sup> and still retained overall image quality. This indicates that with the reduction of electronic noise by PCD technology, applying ultra-low tube potentials to overweight patients may be feasible.

This study has several limitations. Firstly, the radiation doses were estimated rather than directly measured. Secondly, the data are constrained by the absence of a systematic comparison with invasive coronary angiography to evaluate the diagnostic accuracy for coronary stenosis. Thirdly, employing a high-pitch helical scan requires a low and regular heart rate to accommodate the extended image acquisition window and to enable precise triggering of the image capture process. Fourth, the patients



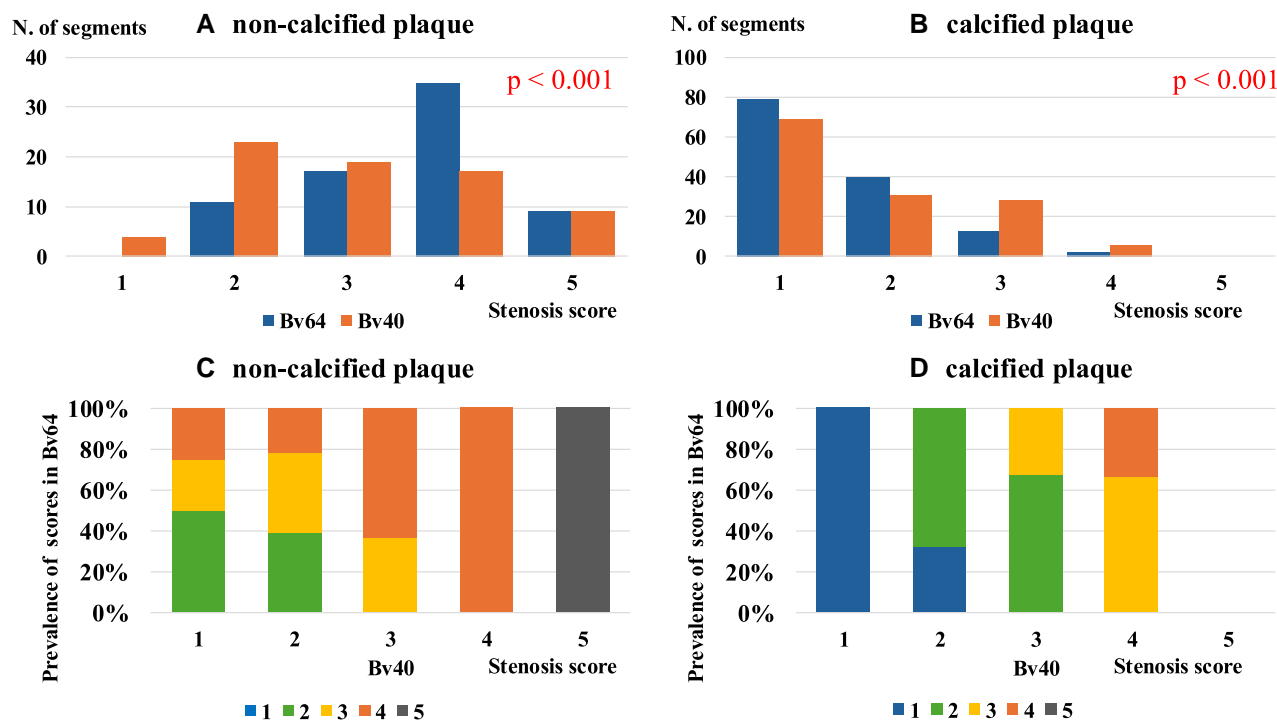


**Figure 6** Per-segment stenosis scores in Bv64 and Bv40 reconstructions. The top two figures show the per-segment stenosis scores for (A) non-calcified plaques ( $n = 72$ ) and (B) calcified plaques ( $n = 134$ ) in Bv64 and Bv40 reconstructions. For non-calcified plaques, the distribution was as follows: score 1 (Bv40:  $n = 4$ , 5.6%; Bv64:  $n = 0$ , 0%), score 2 (Bv40:  $n = 23$ , 31.9%; Bv64:  $n = 11$ , 15.3%), score 3 (Bv40:  $n = 19$ , 26.4%; Bv64:  $n = 17$ , 23.6%), score 4 (Bv40:  $n = 17$ , 23.6%; Bv64:  $n = 35$ , 48.6%), and score 5 (Bv40:  $n = 9$ , 12.5%; Bv64:  $n = 9$ , 12.5%). Similarly, for calcified plaques, the distribution was score 1 (Bv40:  $n = 69$ , 51.5%; Bv64:  $n = 79$ , 59.0%), score 2 (Bv40:  $n = 31$ , 23.1%; Bv64:  $n = 40$ , 29.9%), score 3 (Bv40:  $n = 28$ , 20.9%; Bv64:  $n = 13$ , 9.7%), score 4 (Bv40:  $n = 6$ , 4.5%; Bv64:  $n = 2$ , 1.5%), and score 5 (Bv40:  $n = 0$ , 0%; Bv64:  $n = 0$ , 0%). There was a significant difference in the distribution of stenosis scores between the two kernels for both non-calcified and calcified plaques ( $P < 0.001$ ). The bottom two figures illustrate the changes in stenosis scores between Bv64 and Bv40 kernels for (C) non-calcified plaques ( $n = 72$ ) and (D) calcified plaques ( $n = 134$ ). Specifically, for non-calcified plaques, 41.7% ( $n = 30$ ) increased in stenosis score from Bv40 to Bv64, while 58.3% ( $n = 42$ ) remained the same, and 0% ( $n = 0$ ) decreased. For calcified plaques, 24.6% ( $n = 33$ ) demonstrated a decreased score from Bv40 to Bv64, while 94.0% ( $n = 126$ ) remained the same, and 0% ( $n = 0$ ) increased.

**Table 3** Summary of radiation dose from previous reports and the current study

Authors	CT scanner	Acquisition technique	Tube potential (kVp)	$n$	CTDIvol	DLP	Effective dose	Conversion factor
Lell et al. <sup>22</sup>	Definition Flash	High-pitch helical	100 or 120	25	N.A.	$71 \pm 23$	$1.0 \pm 0.3$	0.014
Achenbach et al. <sup>14</sup>	Definition Flash	High-pitch helical	100	50	N.A.	$62 \pm 5$	$0.87 \pm 0.08$	0.014
Kröpil et al. <sup>13</sup>	Definition Flash	High-pitch helical	80–120	42	N.A.	$99.5 \pm 51.1$	$1.4 \pm 0.7$	0.014
Soschynski et al. <sup>27</sup>	NAEOTOM Alpha	High-pitch helical	120	49	N.A.	N.A.	$1.0 \pm 0.8$	0.015
		Sequential		36	N.A.	N.A.	$4.8 \pm 4.0$	0.015
Rotkopf et al. <sup>25</sup>	NAEOTOM Alpha	High-pitch helical	120	73	$3.0 \pm 1.1$	$56.5 \pm 24.8$	N.A.	N.A.
Rajiah et al. <sup>26</sup>	NAEOTOM Alpha	High-pitch helical	120	53	$2.8 \pm 1.2$	N.A.	N.A.	N.A.
Hoe et al. <sup>28</sup>	NAEOTOM Alpha	Helical (UHR)	120	92	$36.0 \pm 10.7$	$515.6 \pm 171.0$	$7.2 \pm 2.4$	0.014
		Sequential	90	36	$22.6 \pm 8.0$	$307.3 \pm 111.2$	$4.3 \pm 1.6$	0.014
Hagar et al. <sup>29</sup>	NAEOTOM Alpha	Helical (UHR)	120 or 140	68	$67.7 \pm 19.2$	$936 \pm 278$	$13.3 \pm 4.2$	0.014
The current study	NAEOTOM Alpha	High-pitch helical	70	40	$1.72 \pm 0.38$	$29.1 \pm 6.8$	$0.41 \pm 0.09$	0.014
							$0.50 \pm 0.11$	0.017
							$0.82 \pm 0.18$	0.028

CTDIvol, computed tomography dose index volume; DLP, dose-length product; UHR, ultra-high resolution.



enrolled in this study generally had smaller body sizes, which are more commonly observed in Asian populations. Therefore, this ultra-low-dose CCTA protocol may require adjustments when applied to patients with larger body sizes, such as those often seen in European or American populations. Fifth, this study did not utilize invasive coronary angiography, the gold standard for stenosis severity assessment. Consequently, while we observed variations in stenosis severity assessments between the different convolution kernels, the impact of these differences on diagnostic accuracy remains unclear. Further studies employing a reference standard are necessary to clarify the clinical implications of these kernel-dependent assessment variations.

## Conclusion

PCD-CT technology, combined with high-pitch helical scanning and a tube potential of 70 kVp, enabled CCTA to be performed with extremely low radiation exposure (DLP, 29 mGy·cm). The noise reduction capability of PCD-CT allows the use of a sharp kernel even in this low-dose CCTA setting without compromising image quality, potentially improving the evaluation of coronary artery stenosis by reducing the overestimation of stenosis in calcified plaques and the underestimation in non-calcified plaques.

## Supplementary data

Supplementary data are available at *European Heart Journal - Imaging Methods and Practice* online.

## Consent

Written informed consent was waived for the retrospective review of imaging obtained in the course of standard care. All data were thoroughly deidentified before further analyses.

## Funding

None declared.

**Conflict of interest:** Department of Advanced Diagnostic Imaging, where S.N. and K.K. currently belong to, is an endowment department supported with an unrestricted grant from Siemens Healthcare K.K. H.S. receives departmental research grant support from Eisai Co., Ltd, Guerbet Japan KK, FUJIFILM Toyama Chemical Co., Ltd, Nihon Medi-Physics Co., Ltd, PDRadiopharma Inc., and GE Healthcare Japan. All other authors have reported that they have no relationships relevant to the contents of this paper to disclose.

## Data availability

Data supporting the findings of this study are available from the corresponding author (S.N.) upon reasonable request.

## Lead author biography



Dr Satoshi Nakamura is an associate professor and radiologist at the Mie University Hospital. He holds a PhD in radiology and has been actively involved in research on cardiac imaging, with a special focus on coronary artery disease. His research includes the studies of prognosis and diagnostic capabilities related to coronary artery disease using CT and MRI. He continues to advance the field of radiology with his dedication to improving the understanding and application of imaging in cardiac disease.

## References

1. Knuuti J, Wijns W, Saraste A, Capodanno D, Barbato E, Funck-Brentano C *et al.* 2019 ESC guidelines for the diagnosis and management of chronic coronary syndromes. *Eur Heart J* 2020;**41**:407–77.
2. Wolk MJ, Bailey SR, Doherty JU, Douglas PS, Hendel RC, Kramer CM *et al.* ACCF/AHA/ASE/ASNC/HFSA/HRS/SCAI/SCCT/SCMR/STS 2013 multimodality appropriate use criteria for the detection and risk assessment of stable ischemic heart disease. *J Am Coll Cardiol* 2014;**63**:380–406.
3. Budoff MJ, Dowe D, Jollis JG, Gitter M, Sutherland J, Halamert E *et al.* Diagnostic performance of 64-multidetector row coronary computed tomographic angiography for evaluation of coronary artery stenosis in individuals without known coronary artery disease: results from the ACCURACY trial. *J Am Coll Cardiol* 2008;**52**:1724–32.
4. SCOT-HEART investigators. CT coronary angiography in patients with suspected angina due to coronary heart disease (SCOT-HEART): an open-label, parallel-group, multicentre trial. *Lancet* 2015;**385**:2383–91.
5. Newby DE, Adamson PD, Berry C, Boon NA, Dweck MR, Flather M *et al.* Coronary CT angiography and 5-year risk of myocardial infarction. *N Engl J Med* 2018;**379**:924–33.
6. Einstein AJ, Henzlova MJ, Rajagopalan S. Estimating risk of cancer associated with radiation exposure from 64-slice computed tomography coronary angiography. *JAMA* 2007;**298**:317–23.
7. International Commission on Radiological Protection. The 2007 recommendations of the International Commission on Radiological Protection. ICRP publication 103. *Ann ICRP* 2007;**37**:1–332.
8. Hausleiter J, Meyer T, Hermann F, Hadamitzky M, Krebs M, Gerber TC *et al.* Estimated radiation dose associated with cardiac CT angiography. *JAMA* 2009;**301**:500–7.
9. Feuchtner GM, Jodocy D, Klausner A, Haberfellner B, Aglan I, Spöck A *et al.* Radiation dose reduction by using 100-kV tube voltage in cardiac 64-slice computed tomography: a comparative study. *Eur J Radiol* 2010;**75**:e51–6.
10. Gutstein A, Dey D, Cheng V, Wolak A, Gransar H, Suzuki Y *et al.* Algorithm for radiation dose reduction with helical dual source coronary computed tomography angiography in clinical practice. *J Cardiovasc Comput Tomogr* 2008;**2**:311–22.
11. Shuman WP, Branch KR, May JM, Mitsumori LM, Lockhart DW, Dubinsky TJ *et al.* Prospective versus retrospective ECG gating for 64-detector CT of the coronary arteries: comparison of image quality and patient radiation dose. *Radiology* 2008;**248**:431–7.
12. Stolzmann P, Leschka S, Scheffel H, Krauss T, Desbiolles L, Plass A *et al.* Dual-source CT in step-and-shoot mode: noninvasive coronary angiography with low radiation dose. *Radiology* 2008;**249**:71–80.
13. Kröpil P, Rojas CA, Ghoshhajra B, Lanzman RS, Miese FR, Scherer A *et al.* Prospectively ECG-triggered high-pitch spiral acquisition for cardiac CT angiography in routine clinical practice: initial results. *J Thorac Imaging* 2012;**27**:194–201.
14. Achenbach S, Marwan M, Ropers D, Schepis T, Pflederer T, Anders K *et al.* Coronary computed tomography angiography with a consistent dose below 1 mSv using prospectively electrocardiogram-triggered high-pitch spiral acquisition. *Eur Heart J* 2010;**31**:340–6.
15. Sandfort V, Persson M, Pourmorteza A, Noël PB, Fleischmann D, Willemlink MJ. Spectral photon-counting CT in cardiovascular imaging. *J Cardiovasc Comput Tomogr* 2021;**15**:218–25.
16. Leng S, Bruesewitz M, Tao S, Rajendran K, Halaweish AF, Campeau NG *et al.* Photon-counting detector CT: system design and clinical applications of an emerging technology. *Radiographics* 2019;**39**:729–43.
17. Mergen V, Eberhard M, Manka R, Euler A, Alkadhi H. First in-human quantitative plaque characterization with ultra-high resolution coronary photon-counting CT angiography. *Front Cardiovasc Med* 2022;**9**:981012.
18. Leipsic J, Abbara S, Achenbach S, Cury R, Earls JP, Mancini GJ *et al.* SCCT guidelines for the interpretation and reporting of coronary CT angiography: a report of the Society of Cardiovascular Computed Tomography Guidelines Committee. *J Cardiovasc Comput Tomogr* 2014;**8**:342–58.
19. Hausleiter J, Martinoff S, Hadamitzky M, Martuscelli E, Pschierer I, Feuchtner GM *et al.* Image quality and radiation exposure with a low tube voltage protocol for coronary CT angiography: results of the PROTECTION II trial. *JACC Cardiovasc Imaging* 2010;**3**:1113–23.
20. Cury RC, Leipsic J, Abbara S, Achenbach S, Berman D, Bittencourt M *et al.* CAD-RADS™ 2.0 - 2022 Coronary artery disease-reporting and data system: an expert consensus document of the Society of Cardiovascular Computed Tomography (SCCT), the American College of Cardiology (ACC), the American College of Radiology (ACR), and the North America Society of Cardiovascular Imaging (NASCI). *J Cardiovasc Comput Tomogr* 2022;**16**:536–57.
21. Stocker TJ, Deseive S, Leipsic J, Hadamitzky M, Chen MY, Rubinshtein R *et al.* Reduction in radiation exposure in cardiovascular computed tomography imaging: results from the PROTECTION VI registry. *Eur Heart J* 2018;**39**:3715–23.
22. Lell M, Marwan M, Schepis T, Pflederer T, Anders K, Flohr T *et al.* Prospectively ECG-triggered high-pitch spiral acquisition for coronary CT angiography using dual source CT: technique and initial experience. *Eur Radiol* 2009;**19**:2576–83.

23. Rajendran K, Petersilka M, Henning A, Shanblatt ER, Schmidt B, Flohr TG et al. First clinical photon-counting detector CT system: technical evaluation. *Radiology* 2022;**303**:130–8.
24. Si-Mohamed SA, Boccalini S, Lacombe H, Diaw A, Varasteh M, Rodesch PA et al. Coronary CT angiography with photon-counting CT: first-in-human results. *Radiology* 2022;**303**:303–13.
25. Rotkopf LT, Froelich MF, Riffel P, Ziener CH, Reid C, Schlemmer HP et al. Influence of heart rate and heart rate variability on the feasibility of ultra-fast, high-pitch coronary photon-counting computed tomography angiography. *Int J Cardiovasc Imaging* 2023;**39**:1065–73.
26. Rajiah PS, Dunning CAS, Rajendran K, Tandon YK, Ahmed Z, Larson NB et al. High-pitch multienergy coronary CT angiography in dual-source photon-counting detector CT scanner at low iodinated contrast dose. *Invest Radiol* 2023;**58**:681–90.
27. Soschynski M, Hagen F, Baumann S, Hagar MT, Weiss J, Krauss T et al. High temporal resolution dual-source photon-counting CT for coronary artery disease: initial multicenter clinical experience. *J Clin Med* 2022;**11**:6003.
28. Hoe J, Toh KH. Initial clinical experience with coronary CT angiography performed on dual source photon counting CT using different cardiac scan modes-analysis of image quality and radiation dose. *Cardiovasc Imaging Asia* 2023;**7**:39–48.
29. Hagar MT, Soschynski M, Saffar R, Rau A, Taron J, Weiss J et al. Accuracy of ultrahigh-resolution photon-counting CT for detecting coronary artery disease in a high-risk population. *Radiology* 2023;**307**:e223305.
30. LaBounty TM, Leipsic J, Poulter R, Wood D, Johnson M, Srichai MB et al. Coronary CT angiography of patients with a normal body mass index using 80 kVp versus 100 kVp: a prospective, multicenter, multivendor randomized trial. *AJR Am J Roentgenol* 2011;**197**:W860–7.
31. Oda S, Utsunomiya D, Funama Y, Yonenaga K, Namimoto T, Nakaura T et al. A hybrid iterative reconstruction algorithm that improves the image quality of low-tube-voltage coronary CT angiography. *AJR Am J Roentgenol* 2012;**198**:1126–31.
32. Mangold S, Wichmann JL, Schoepf UJ, Poole ZB, Canstein C, Varga-Szemes A et al. Automated tube voltage selection for radiation dose and contrast medium reduction at coronary CT angiography using 3rd generation dual-source CT. *Eur Radiol* 2016;**26**:3608–16.